Postprint of: Pietrzak P., Meller M., Niedźwiecki M., Dynamic mass measurement in checkweighers using a discrete time-variant low-pass filter, MECHANICAL SYSTEMS AND SIGNAL PROCESSING, Vol. 48, iss. 1-2 (2014), pp. 67-76, DOI: 10.1016/j.ymssp.2014.02.013

Dynamic mass measurement in checkweighers using a discrete time-variant low-pass filter

Przemysław Pietrzak[a,*], Michał Meller[b], Maciej Niedźwiecki[b]

[a]*Department of Control and Measurement, West Pomeranian University of Technology, Sikorskiego 37, 70-313 Szczecin, Poland*
[b]*Department of Automatic Control, Faculty of Electronics, Telecommunications and Informatics, Gdańsk University of Technology, Narutowicza 11/12, 80-233 Gdańsk, Poland*

Abstract

Conveyor belt type checkweighers are complex mechanical systems consisting of a weighing sensor (strain gauge load cell, electordynamically compensated load cell), packages (of different shapes, made of different materials) and a transport system (motors, gears, rollers). Disturbances generated by the vibrating parts of such a system are reflected in the signal power spectra in a form of strong spectral peaks, located usually in the lower frequency range. Such low frequency components overlap in the frequency domain with the useful signal and it is very difficult to eliminate them. The conventional way of suppressing disturbances is via low-pass filtering of the signal obtained from the load cell. However, if the speed of of the conveyor belt is high, the response of the applied filter may not settle fast enough to enable accurate weighing of objects in motion, i.e., without stopping them on the weighing conveyor. Since attempts to overcome this problem using classical linear time-invariant low-pass filtering fail for high belt speeds, the paper presents and verifies experimentally a new approach, based on time-variant low-pass filtering. It is shown that, when properly tuned, the proposed time-variant filter fulfills the measurement accuracy requirements for a wide range of operating conditions.

Keywords: Dynamic mass measurement, automatic weighing, conveyor belt type checkweigher, time-variant low-pass filter, signal processing, mechanical vibrations.

1. Introduction

In industrial fields it is often necessary to weigh objects in motion, without stopping them on the weighing platform. Fast weighing, i.e., weighing in a time that is much shorter than the settling time of the measuring instrument, is one of the basic challenges in the field of dynamic mass measurement [1]. Dynamic weighing systems are usually used to check quantities of pre-packaged products. In this group of applications the conveyor belt type checkweighers play an increasingly important role [2].

Checkweighers belong to a group of automatic catchweighing instruments [3]. They are mostly a part of production lines and are integrated into a load transport system. During normal operation the transported products are moved sequentially along the weighing conveyor and weighed on-the-fly without any intervention of an operator, as it is schematically depicted in Fig. 1. The main source of disturbances corrupting the measurement signal, reflected in the signal power spectra in a form of well-emphasized spectral peaks (located usually in the lower frequency range, from several up to tens of Hz) are mechanical vibrations [4], [5], [6], [7], [8],[9]. The disturbance spectrum varies with the conveyor belt speed and the mass of the weighed object. Moreover, such low frequency components overlap in the frequency domain with the useful signal and it is practically impossible to eliminate them completely. For this reason some more advanced noise attenuation techniques must be used [10], [11].

*Corresponding author
Email addresses: pietrzak@zut.edu.pl (Przemysław Pietrzak), michal.meller@eti.pg.gda.pl (Michał Meller), maciekn@eti.pg.gda.pl (Maciej Niedźwiecki)

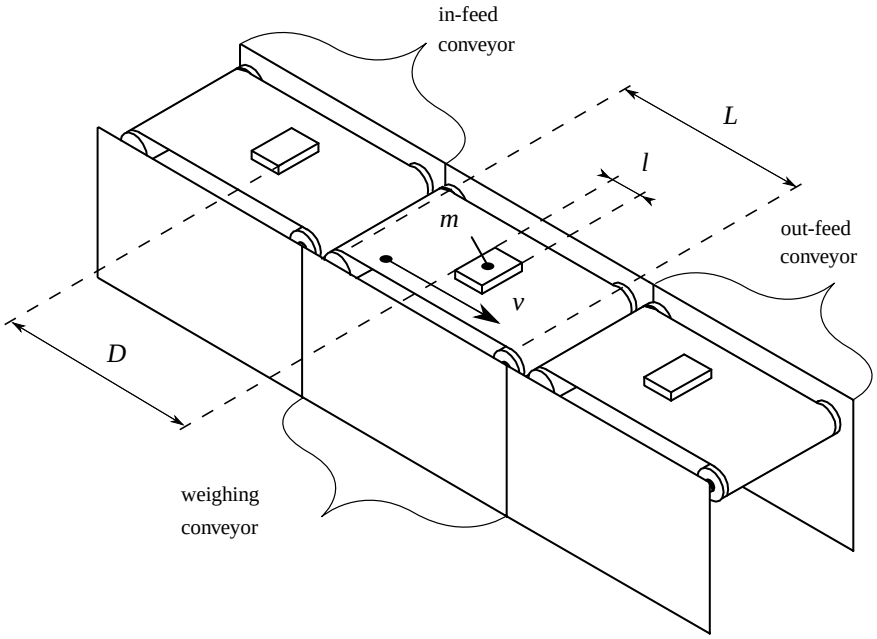

(a) a conveyor belt type checkweigher

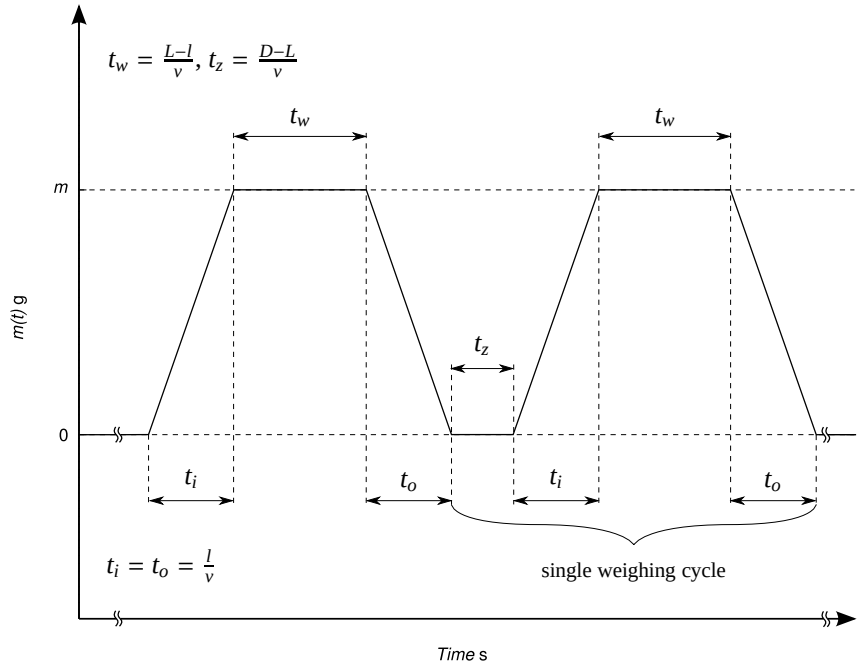

(b) weighing cycle of a conveyor belt type checkweigher

Figure 1: A conveyor belt type checkweigher and its weighing cycle. L is the length of the weighing conveyor, l and m denote respectively the active length and the mass of the weighed object, D is the distance between two consecutive objects, and v denotes the belt speed.

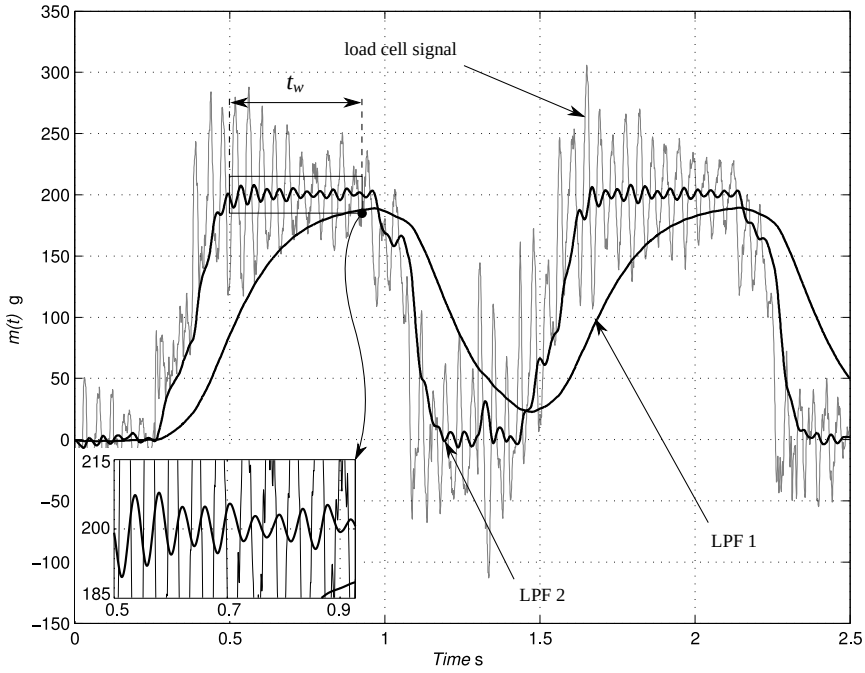

Figure 2: The fundamental limitation of linear time-invariant low-pass filtering: the length of a transient response of the filter with low cutoff frequency (LPF 1) exceeds the length of the weighing period t_w. On the other hand, the response of a filter with high cutoff frequency (LPF 2) exhibits significant oscillations during the weighing period.

The paper solves the above-mentioned problem by proposing and verifying experimentally a linear time-variant low-pass filtering technique. The new solution is compared with the identification-based approach proposed earlier in the literature [12],[13] and with the classical filtering approach incorporating time-invariant low-pass filters.

2. Problem formulation

Suppose that to eliminate disturbances, one performs linear low-pass filtering of the measured signal. Narrowing the filter passband decreases the influence of disturbances and increases the measurement accuracy. However, bandwidth limitation is always achieved at the expense of increasing the settling time of a filter. In extreme cases the duration of the filter transient may even exceed the duration of the weighing period. Improving the transient response is possible by extending the filter bandwidth, this however increases the amplitude of disturbances occurring during the weighing stage, as shown in Fig. 2. Both scenarios mentioned above illustrate the fundamental limitation of time-invariant filtering: for a linear time-invariant low-pass filter the requirements of short transient response and high disturbance attenuation are contradictory - modifying the filter passband, one always improves one filter characteristic at the expense of the other. As a result it is not possible to achieve high measurement accuracy.

In order to reduce the length of the transient response of the filter, a bank of two or more low-pass filters with complementary properties, combined into a switched parallel structure, was proposed in [6]. According to the Authors, in such a scheme at least one filter with low cutoff frequency (i.e., long transient response) and one filter with high cutoff frequency (i.e., short transient response) should be used. In the proposed solution two complementary moving average FIR filters and a simplified Kalman filter were utilized; switching between filters was based on steady-state criteria and realized in a way that does not produce discontinuities in the output signal.

Another way of attaining reduction in the duration of the filter transient response, worked out for analog low-pass filters, was pointed out in [14], [15]. The goal was achieved by varying the values of the filter coefficients in the time interval where the transient behavior is expected to occur. Coefficient changes were related to changes in the cutoff

frequency. In the initial phase of filtering a constant-high cutoff frequency was used; later on it was decreased, in a continuous manner, until it reached a prescribed terminal value.

Leaving aside the fact that the method presented in [6] was designed for discrete-time signals, while the method proposed in [14], [15] – for continuous-time signals, by comparing them one can find the following analogy: in both cases the properties of the filter vary with time. There are also some important differences. In the first case parameters of individual filters are fixed, yet - due to switching between them - the internal system structure changes over time. In the second case, filter parameters are subject to continuous changes, while the filter structure remains unchanged. In both cases, however, time-variability of the filter allows one to reduce the duration of its transient response. This suggests that using a time-variant filter, one should be able to achieve the desired level of disturbance attenuation without increasing the length of the filter transient.

3. Discrete time-variant low-pass filter

3.1. The analysis interval

A typical weighing cycle consists of the input stage, of length t_i, during which the weighed object gradually slides on the weighing conveyor, weighing stage, of length t_w, during which the entire object remains on the weighing conveyor, and the output stage, of length $t_o = t_i$, during which the object slides of the conveyor - see Fig. 1(b). The beginning and the end of each stage can be easily determined using signals from photocells located between the in-feed and weighing conveyor, and between the weighing and out-feed conveyor, as shown in Fig. 3. The time interval covering both the input stage and the weighing stage will be further referred to as the analysis interval. Note that the length of the analysis interval is given by $t_i + t_w = v^{-1}L$, where L denotes the length of the weighing conveyor and v denotes its speed, and hence it does not depend on the active length l of the weighed object. The samples of the load cell signal, measured in the analysis interval, will be further denoted by

$$x(1),\ x(2),\ x(3),\ \ldots,\ x(N), \tag{1}$$

where the first element, with index 1, precedes the rising edge of the front photocell pulse and the last element, with index N, precedes the rising edge of the end photocell pulse. Our estimates of the object mass will be obtained by means of processing the sequence (1).

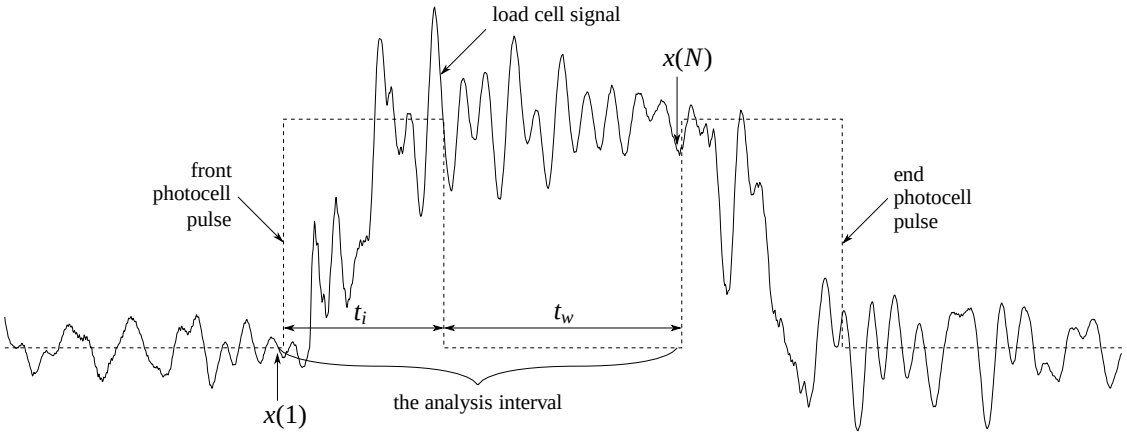

Figure 3: Typical responses of the load cell (solid line) and both photocell signals (dotted lines) observed during a single weighing cycle. Curly bracket shows localization of the analysis interval.

3.2. Filter synthesis

One possible approach, widely used in industrial applications [9], is to determine the static weight of the object based on the analysis of the lowpass-filtered load cell signal. Good results (see [16] and Section 4 below) can be

achieved using a cascade connection of the first-order IIR filters of the form

$$y_i(n) + a_k y_i(n-1) = b_k\Big[y_{i-1}(n) + y_{i-1}(n-1)\Big], \tag{2}$$

$$i = 1, \ldots, k, \quad n = 1, \ldots, N\,,$$

where k denotes the number of filters making up a cascade. The input signal entering the cascade is taken from the load cell, i.e., $y_0(n) = x(n)$, and the weight estimate is obtained by reading out the signal observed at the output of the cascade at the instant N

$$\widehat{m}(N) = y_k(N). \tag{3}$$

When the order-dependent filter coefficients a_k and b_k (the same for all filters making up a cascade) are chosen according to

$$a_k = \frac{f_c - \frac{c_k}{\pi\Delta}}{f_c + \frac{c_k}{\pi\Delta}}\,, \quad b_k = \frac{1 + a_k}{2}\,, \quad c_k = \sqrt{\sqrt[k]{2} - 1}, \tag{4}$$

where Δ [s] denotes the sampling period and f_c [Hz] denotes the desired cutoff frequency, equations (2) can be regarded as a discrete approximation of an analog critically damped low-pass filter.

Further improvement can be achieved by using time-variant low-pass filters governed by

$$y_i(n) + a_k(n) y_i(n-1) = b_k(n)\Big[y_{i-1}(n) + y_{i-1}(n-1)\Big] \tag{5}$$

$$i = 1, \ldots, k, \quad n = 1, \ldots, N\,,$$

where $a_k(n)$ and $b_k(n)$ denote time-varying coefficients obtained from (2) after replacing the time-invariant cutoff frequency f_c with its time-varying counterpart $f_c(n)$. Even though for a time-variant filter the cutoff frequency is a heuristic concept, difficult to justify in a mathematically strict manner, when used with a due caution it can be very helpful in designing filters with improved characteristics. In our current context the idea is to use a filter with a relatively large bandwidth at the initial stage of filtration (i.e., during the input stage), and to gradually reduce the bandwidth as the end of the analysis interval (i.e., the end of the weighing stage) is approached. Such bandwidth scheduling allows one to obtain low-pass filters with a shorter transient response compared to response of time-invariant filters characterized by the same level of disturbance attenuation. To achieve this goal, the time-varying "cutoff frequency" $f_c(n)$ was parameterized as follows (see Fig. 4)

$$f_c(n) = f_\infty + (f_0 - f_\infty)\lambda^{\frac{n-1}{\alpha(N-1)}}, \tag{6}$$

where $\lambda = 0.01$ is a small real number, $f_\infty < f_0$, and α denotes the decay rate. According to (6), in the interval $[1, N]$ the cutoff frequency $f_c(n)$ decreases monotonically from the initial value $f_c(1) = f_0$ towards the limiting value f_∞, with a speed depending on the parameter α. Note that for $\alpha = 1$ it holds that $f_c(N) = (1-\lambda) f_\infty + \lambda f_0 \cong f_\infty$, i.e., the cutoff frequency at the end of the analysis interval is close to f_∞.

3.3. Optimal filter settings

The parameter f_∞ of the function (6) and the cascade order k characterize a time-invariant filter, to which the filter (5) converges when the time variable n tends to infinity. Both parameters can be selected by analyzing the magnitude of the Fourier transform components of (1), e.g. by using the multiple time averaging method [11]. The parameters f_0 and α determine the time-varying behaviour of the filter (5). Their optimal values were found, using the Nelder–Mead simplex method [17], by means of minimizing – for each of nine belt speeds v_j, $j = 1, \ldots, 9$ – the performance measure made up of two components

$$\boldsymbol{\xi}_j^* = \arg\min_{\boldsymbol{\xi}} \Big\{\delta_j(\boldsymbol{\xi}) + \eta_j(\boldsymbol{\xi})\Big\}, \quad \boldsymbol{\xi} = [f_0, \alpha]^{\mathrm{T}} \in \mathbb{R}^2, \tag{7}$$

subject to the constraints

$$f_0 \geqslant f_\infty, \ \alpha \geqslant 1. \tag{8}$$

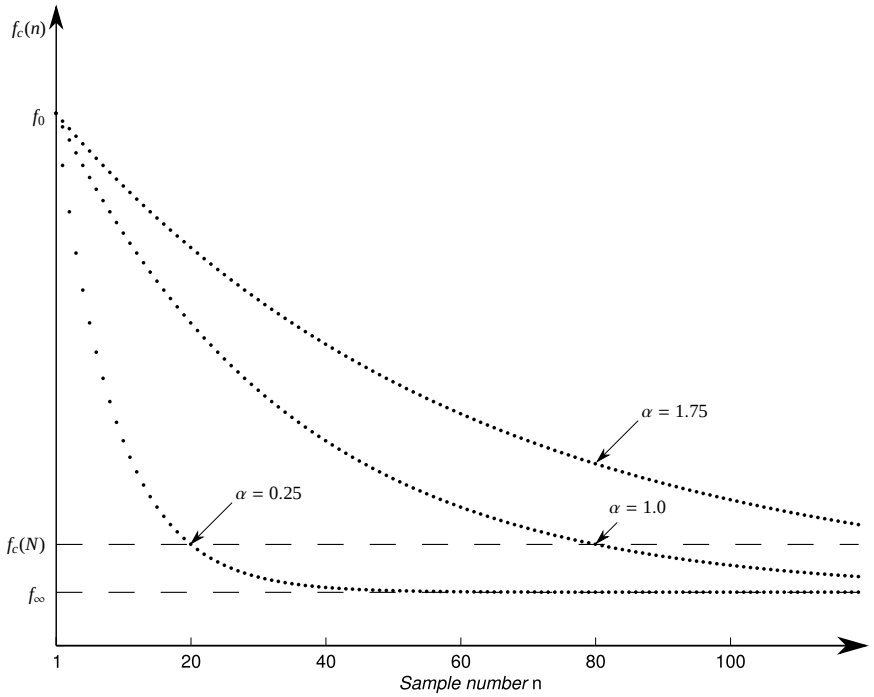

Figure 4: Plots of the function $f_c(n) = f_\infty + (f_0 - f_\infty)\lambda^{\frac{n-1}{\alpha(N-1)}}$ for $N = 80$, $\lambda = 0.1$, and 3 different values of α.

The first component of the function (7) quantifies the measurement accuracy, taking into account metrological recommendations

$$\delta_j(\boldsymbol{\xi}) = \max\left\{\frac{\mu_{ij}(\boldsymbol{\xi})}{\mu_{i\max}}\,,\frac{\sigma_{ij}(\boldsymbol{\xi})}{\sigma_{i\max}}\,,\ i=1,\ldots,3\right\} \tag{9}$$

where $\mu_{ij}(\boldsymbol{\xi})$ and $\sigma_{ij}(\boldsymbol{\xi})$ denote the mean error values and standard error deviations computed for the i-th test load m_i ($i = 1,\ldots,3$) and the j-th conveyor belt speed v_j ($j = 1,\ldots,9$) based on the training data set. The quantities $\mu_{i\max}$ and $\sigma_{i\max}$ denote the corresponding maximum permissible values (listed in Table 1) set in accordance with the requirements specified in [3] for the category XIII(1) instruments. For a given belt speed v_j the quantities $\mu_{ij}(\boldsymbol{\xi})$ and $\sigma_{ij}(\boldsymbol{\xi})$ were evaluated using the set of 20 independent mass measurements collected for each test load m_i, $i = 1,\ldots,3$. According to (3), the corresponding measurement errors were defined as $e_{ij}^l(\boldsymbol{\xi}) = m_i - \widehat{m}_{ij}^l(N|\boldsymbol{\xi})$, where the superscript l, $l = 1,\ldots,20$, denotes the measurement number.

The second component of the performance measure (7) penalizes long transient responses and is given by

$$\eta_j(\boldsymbol{\xi}) = \max\left\{\frac{n_{ij}(\boldsymbol{\xi})}{N}\,,\ i=1,\ldots,3\right\} \tag{10}$$

where $n_{ij}(\boldsymbol{\xi}) \in [1, N]$ denotes the smallest time coordinate n, starting from which the output of the filter (5) yields mass measurements $\widehat{m}_{ij}(n|\boldsymbol{\xi}) = y_k(n)$ that comply with the accuracy specifications summarized in Table 1. Note that when $n_{ij}(\boldsymbol{\xi}) < N$, then not only the last sample $y_k(N)$, but also a certain number of previous filter response samples can be used as weight estimates without violating the accuracy requirements. If for the last sample of the filter response $y_k(N)$ it holds that $|\mu_{ij}(\boldsymbol{\xi})| > \mu_{i\max}$ or $\sigma_{ij}(\boldsymbol{\xi}) > \sigma_{i\max}$, the value of $\eta_j(\boldsymbol{\xi})$ is set to 1. Inclusion of $\eta_j(\boldsymbol{\xi})$ in (7) increases robustness of the filter to anomalous data.

3.4. Continuous operation

During normal operation of the checkweigher, the time-variant filter works in a continuous manner, cyclically switching between the static mode and the dynamic mode. The static mode, enabled by setting the f_c parameter to

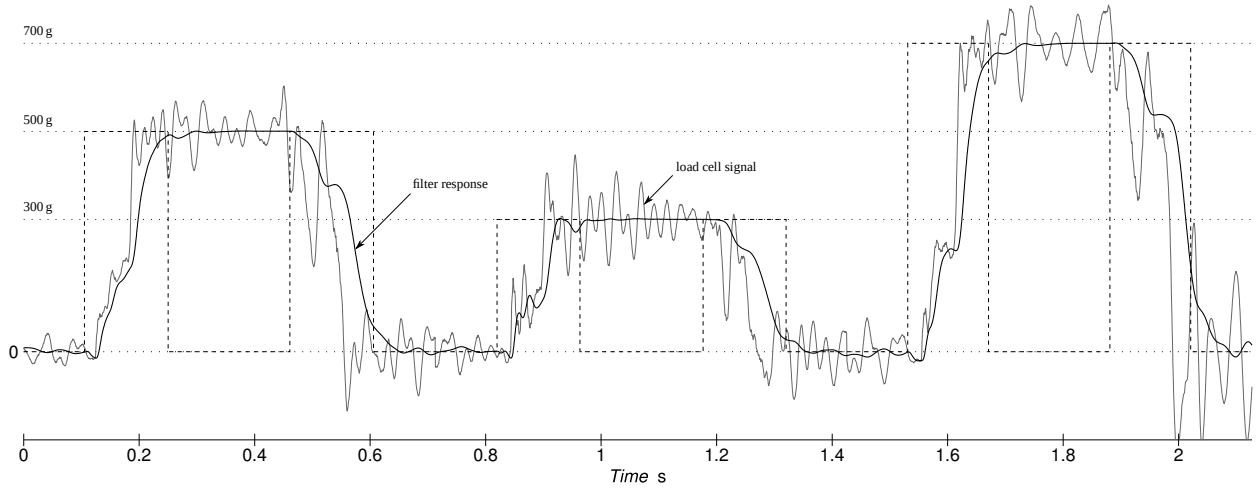

(a) filter response against the load cell signal

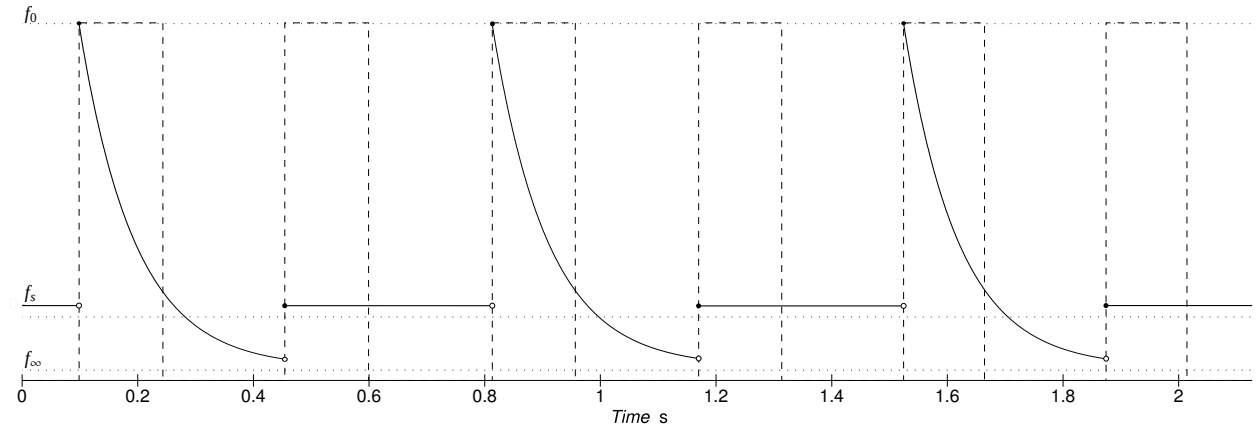

(b) evolution of the cutoff frequency $f_c(n)$

Figure 5: Continuous operation of the proposed time-variant filter.

a constant value f_s, is a default operating regime of the system; it is activated during the start-up of the weighing module and lasts until the rising edge of the signal from the photocell located between the in-feed and the weighing conveyor is detected – see Fig. 5. The value of f_s should be chosen in such a way that the measurement error in the static mode does not exceed permissible values, specified by the recommendation [18]. Detection of the rising edge at the output of the first photocell triggers the dynamic mode of the filter, which lasts until the rising edge at the output of the second photocell is detected. Then the current value of the filter output, treated as a mass measurement, is read out and the filter returns to the static mode. At all time instants n, including the moments of switching between the static mode and dynamic mode, the system works in a fully autonomous way, i.e., the filtration is governed by the equation (5), and filter parameters are calculated according to (4) based on the current value of the cutoff frequency $f_c(n)$.

4. Experimental Verification

All experiments were carried out using an instrument shown in Fig. 6, made up of three conveyor belts. The length of the weighing conveyor (mounted on a strain gauge load cell) was equal to $L = 350$ mm. The basic facts about the

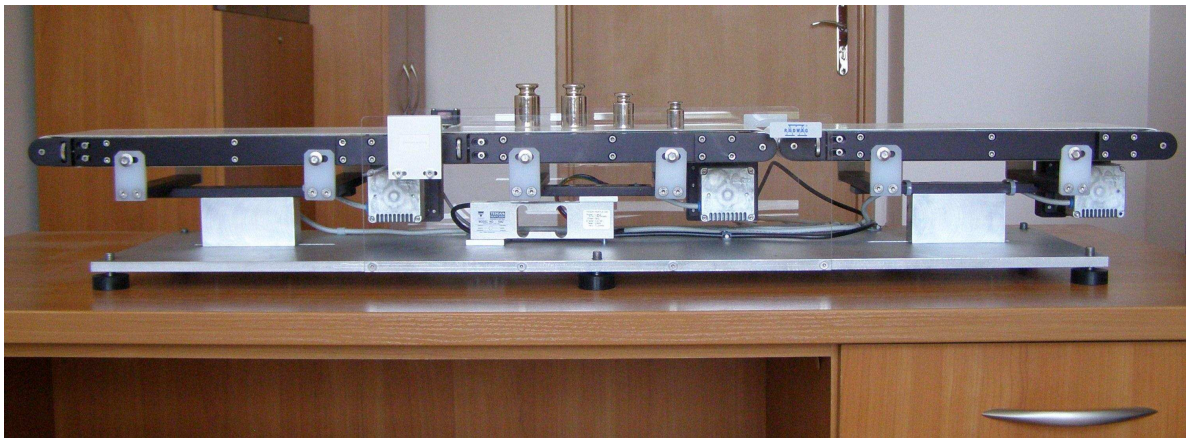

Figure 6: The experimental test-stand.

Length L of the weighing conveyor			350 mm	
Conveyor speed range v			0.5 – 1.3 $\frac{\text{m}}{\text{s}}$	
Test load i	Mass m_i	Active length l_i	$\mu_{i\max}$	$\sigma_{i\max}$
1	300 g			0.48 g
2	500 g	142 mm	0.5 g	0.8 g
3	700 g			0.8 g

Table 1: Specification of experimental conditions, test loads, and the XIII(1) accuracy class maximum permissible values of $\mu_{i\max}$ and $\sigma_{i\max}$.

experimental conditions, test loads, and the desired accuracy specifications are summarized in Table 1. For each of three test loads and each of nine belt speeds (ranging from 0.5 to 1.3 $\frac{\text{m}}{\text{s}}$, in steps of 0.1 $\frac{\text{m}}{\text{s}}$), twenty consecutive test weighings were performed. After applying the above procedure twice, two sets of measurements were acquired. The first set was used for training purposes, i.e., to optimize filter settings according to (7). The performance evaluation was made using the second set. In all cases the signals obtained from the load cell and two photocells were sampled at the rate of 1.6 kHz and stored on the computer hard disk. The length N of the analysis interval varied from 1085 samples for $v = 0.5\ \frac{\text{m}}{\text{s}}$ to 424 samples for $v = 1.3\ \frac{\text{m}}{\text{s}}$.

4.1. Filtration-based approach

In this approach a static weight of the test load was determined based on analysis of the filtered load cell signal. Three filters were compared: classical discrete-time time-invariant Bessel filter, time-invariant critically damped filter (2), and time-variant filter (5) operated in a continuous mode.

Optimal filter settings $\boldsymbol{\xi}_j^*$ were obtained by means of minimizing the performance measure (7) for a training data set. For time-invariant filters, optimal settings were found by searching a discretized space of parameters $\boldsymbol{\xi} = [k,\ f_c]^{\text{T}}$, where k denotes the filter order and f_c denotes the cutoff frequency. In the case of the time-variant filter, the algorithm described in subsection 3.3 was used. The results of optimization are summarized in Table 2. The verification results, obtained using the evaluation data set (i.e., the one that was not used for optimization purposes), are presented in Table 3.

4.2. Identification-based approach

The identification-based approach to dynamic weighing is based on different principles. Within this approach it is assumed that the signal $x(n)$ observed at the output of the checkweigher at the weighing stage can be modeled as a response of an unknown dynamic system to a constant excitation signal $u(n)$ (under nonzero initial conditions) [12], [13]. In a number of publications, to describe the dynamics of the load cell or even of the entire checkweigher,

$v\left[\frac{\mathrm{m}}{\mathrm{s}}\right]$	0.5	0.6	0.7	0.8	0.9	1.0	1.1	1.2	1.3
time-invariant Bessel filter									
f_c^*	5.7	5.4	7.6	8.4	7.2	8.1	8.9	9.2	9.6
k^*	13	10	13	12	7	7	10	7	9
time-invariant critically damped filter									
f_c^*	2.5	2.7	3.0	3.4	3.5	3.7	4.1	4.3	4.4
k^*	18	19	14	17	13	13	14	12	8
time-variant filter									
f_0^*	66.5	48.0	49.0	26.0	35.5	35.0	39.0	32.0	32.5
f_∞^*					0.01				
α^*	0.86	0.97	0.99	1.29	1.16	1.20	1.18	1.37	1.33
k^*					3				

Table 2: Optimal filter settings $\boldsymbol{\xi}_j^*$ for different conveyor belt speeds.

a simple model of damped harmonic oscillator was used [5], [15], [19], [20], [21], [22], [23]. The discrete-time description of such a system takes the form

$$X(z) = H(z)U(z), \quad H(z) = \frac{bz^{-1}}{1 + a_1 z^{-1} + a_2 z^{-2}} \tag{11}$$

where $X(z)$ and $U(z)$ denote $\mathcal{Z}$-transforms of the input and output sequences, respectively, and $H(z)$ denotes the system transfer function.

Assuming that the input signal is constant, namely $u(n) \equiv u_0 > 0$, the steady state value of the output signal (equal to the mass of the weighed object) may be computed using the final value theorem, according to which

$$x(\infty) = \frac{bu_0}{1 + a_1 + a_2} \ . \tag{12}$$

The indirect mass measurement may be accomplished by means of estimating – using the available output signal (1) – the values of the coefficients appearing in (11), and applying (12). Denote by n_0 the time coordinate of the falling edge of the front photocell pulse (which corresponds to the beginning of the weighing stage). Incorporating the method of least squares, one obtains

$$\widehat{\boldsymbol{\theta}}(N) = [\boldsymbol{\Phi}^{\mathrm{T}}(N)\boldsymbol{\Phi}(N)]^{-1}\boldsymbol{\Phi}^{\mathrm{T}}(N)\mathbf{x}(N) \tag{13}$$

where $\widehat{\boldsymbol{\theta}}(N) = [\widehat{b}(N), \widehat{a}_1(N), \widehat{a}_2(N)]^{\mathrm{T}}$ denotes the vector of estimates of system parameters, $\boldsymbol{\Phi}(N) = [\boldsymbol{\phi}(n_0), \ldots, \boldsymbol{\phi}(N)]^{\mathrm{T}}$ is the matrix made up of regression vectors $\boldsymbol{\phi}(n) = [u_0, -x(n-1), -x(n-2)]^{\mathrm{T}}$, $n = n_0, \ldots, N$, and $\mathbf{x} = [x(n_0), \ldots, x(N)]^{\mathrm{T}}$. The mass estimate can be obtained from

$$\widehat{m}(N) = \frac{\widehat{b}(N)u_0}{1 + \widehat{a}_1(N) + \widehat{a}_2(N)} \ . \tag{14}$$

It is worth noting that for the method to work, the amplitude of the input signal u_0 (the true value of u_0, proportional to the mass of the weighed object, is unknown) may be chosen arbitrarily, e.g. one can set $u_0 = 1$. This is because variations in the assumed input signal amplitude are automatically compensated by the corresponding changes in $\widehat{b}(N)$ – see [12]. Since the identification-based approach operates in an adaptive way, there is no need to use the training data set. The verification results for this approach, obtained using the evaluation data set, are presented in Table 4.

4.3. Verification summary

The presented results show clearly advantages of the new method in terms of the measurement accuracy. While the classical time-invariant filters offer reasonably good results but fail at speeds in excess of 0.9 $\frac{\mathrm{m}}{\mathrm{s}}$, the proposed method

$v\left[\frac{\mathrm{m}}{\mathrm{s}}\right]$	0.5	0.6	0.7	0.8	0.9	1.0	1.1	1.2	1.3
time-invariant Bessel filter									
μ_{1j}	-0.03	-0.12	-0.01	-0.01	-0.14	-0.25	0.15	-0.25	-0.27
σ_{1j}	0.16	0.05	0.16	0.13	0.15	0.23	0.20	0.31	0.24
μ_{2j}	0.09	-0.10	0.03	0.21	-0.29	**-0.51**	0.25	0.06	-0.04
σ_{2j}	0.11	0.13	0.14	0.16	0.12	0.21	0.13	0.33	0.25
μ_{3j}	-0.03	0.25	-0.14	0.34	-0.28	0.01	-0.47	**1.23**	**0.59**
σ_{3j}	0.14	0.13	0.17	0.13	0.25	0.32	0.18	0.50	0.36
time-invariant critically damped filter									
μ_{1j}	-0.15	-0.08	-0.09	-0.15	-0.20	-0.24	-0.16	-0.07	-0.47
σ_{1j}	0.14	0.07	0.16	0.14	0.18	0.24	0.25	0.25	0.51
μ_{2j}	-0.05	0.08	-0.10	0.03	-0.15	-0.46	0.35	0.24	**-0.53**
σ_{2j}	0.12	0.15	0.14	0.22	0.19	0.24	0.34	0.37	0.71
μ_{3j}	0.13	0.14	0.18	0.34	-0.08	**-0.68**	-0.39	**-0.54**	**-1.41**
σ_{3j}	0.13	0.15	0.17	0.11	0.25	0.27	0.47	**0.90**	**0.90**
time-variant filter									
μ_{1j}	-0.10	-0.06	-0.03	-0.12	-0.07	-0.05	0.10	-0.10	-0.26
σ_{1j}	0.14	0.05	0.13	0.10	0.12	0.13	0.14	0.13	0.14
μ_{2j}	0.02	0.04	0.01	-0.09	-0.05	-0.13	0.30	-0.28	-0.34
σ_{2j}	0.12	0.12	0.11	0.14	0.10	0.13	0.11	0.16	0.17
μ_{3j}	0.04	0.07	0.11	-0.19	-0.08	-0.14	0.36	-0.23	-0.41
σ_{3j}	0.13	0.10	0.15	0.12	0.17	0.13	0.12	0.22	0.22

Table 3: Mean errors $\mu_{ij}(\boldsymbol{\xi}_j^*)$ and their standard deviations $\sigma_{ij}(\boldsymbol{\xi}_j^*)$ for the i-th test load and the j-th conveyor belt speed in the filtration-based approach. The values that exceed the accuracy XIII(1) specifications (given in Table 1) are shown in boldface.

$v\left[\frac{\mathrm{m}}{\mathrm{s}}\right]$	0.5	0.6	0.7	0.8	0.9	1.0	1.1	1.2	1.3
μ_{1j}	**1.78**	0.10	-0.43	**1.06**	**1.53**	**2.91**	**3.46**	**0.4**	**2.64**
σ_{1j}	0.70	**0.82**	**1.25**	**1.97**	**1.07**	**2.32**	**2.75**	**3.33**	**1.96**
μ_{2j}	-0.09	-0.11	-0.12	**-3.29**	**1.58**	**4.02**	**4.22**	**1.29**	**7.84**
σ_{2j}	**2.41**	**0.91**	**1.09**	**5.13**	**2.16**	**3.62**	**4.88**	**2.86**	**3.25**
μ_{3j}	-0.21	**0.59**	**1.39**	**0.98**	0.24	0.23	**5.49**	**10.15**	**0.83**
σ_{3j}	**1.18**	**1.52**	**1.68**	**4.06**	**2.22**	**2.14**	**2.85**	**6.39**	**3.72**

Table 4: Experimental results obtained for the identification-based approach.

yields satisfactory results under all operating conditions. Unlike the filtering-based methods, the identification-based approach incorporating the second-order mass-spring-damper model fails for all test loads and all belt speeds.

The computational burden of the proposed approach is low. The cost of the Nelder-Mead algorithm, which belongs to the class of direct search methods, depends mainly on the objective function, the starting point and the initial simplex size. For this class of methods the criterion corresponding to an average number of objective function executions seems to be a right choice. As it was found, for all optimization tasks (7), performed for nine considered belt speeds v, the average number of evaluated vertices did not exceed 100. It should be noted, however, that since the optimization step is performed in the offline mode, the optimization cost is incurred only once. The online part of the filtration routine, governed by (5), requires $3Nk$ multiply-add operations, i.e., in the case considered, only 9 operations are needed per time update.

5. Conclusions

In spite of the presence of strong low-frequency disturbances, the proposed linear discrete time-variant low-pass filter is able to ensure that for a wide range of conveyor belt speeds the measurement errors do not exceed their permissible values. The problem considered in the introduction can therefore be considered as successfully solved. The cascade connection of k first-order filters (5) can be easily implemented in a floating point microprocessor-based system. Given the number of arithmetic operations that are needed per time update, the computational cost of the filter is negligible. If the problem of finding the optimal filter design is formulated in a more general way, with relaxed constraints put on the sequence (6), some further improvements can be expected. The future work should provide more insight into this issue.

Aknowledgments

The authors would like to thank RADWAG Wagi Elektroniczne for their support and expert help.

References

[1] T. Yamazaki, T. Ono, Dynamic problems in measurement of mass-related quantities, in: Proc. SICE, 2007, pp. 1183–1188.
[2] R. Schwartz, Automatic weighing-principles, applications and developments, in: Proc. XVI IMEKO, 2000, pp. 259–267.
[3] International recommendation OIML R 51-1, Automatic catchweighing instruments. Part 1: Metrological and technical requirements - Test (2006).
[4] M. Tariq, W. Balachandran, S.Song, Checkweigher modelling using dynamical subsystems, in: Proc. IEEE IAS, Vol. 2, 1995, pp. 1715–1722.
[5] G. Boschetti, R. Caracciolo, D. Richiedei, A. Trevisani, Model-based dynamic compensation of load cell response in weighing machines affected by environmental vibrations, Mechanical Systems and Signal Processing 34 (12) (2013) 116 – 130.
[6] R. Maier, G. Schmidt, Integrated digital control and filtering for an electrodynamically compensated weighing cell, IEEE Trans. Instrum. Meas. 38 (5) (1989) 998–1003.
[7] T. Yamazaki, Y. Sakurai, H. Ohnishi, M. Kobayashi, S. Kurosu, Continuous mass measurement in checkweighers and conveyor belt scales, in: Proc. SICE, Vol. 1, 2002, pp. 470–474.
[8] K. Fukuda, K. Yoshida, T. Kinugasa, M. Kamon, Y. Kagawa, T. Ono, A new method of mass measurement for checkweighers, Metrology and Measurement Systems XVII (2) (2010) 151–162.
[9] M. McGuinness, D. Jenkins, G. Senaratne, Modelling the physics of high-speed weighing, Tech. rep., Mathematics in Industry Information Service (2005).
[10] R. Tasaki, T. Yamazaki, H. Ohnishi, M. Kobayashi, S. Kurosu, Continuous weighing on a multi-stage conveyor belt with FIR filter, Measurement 40 (7-8) (2007) 791–796.
[11] M. Halimic, W. Balachandran, Kalman filter for dynamic weighing system, in: Proc. IEEE ISIE, Vol. 2, 1995, pp. 786–791.
[12] M. Niedźwiecki, A. Wasilewski, Application of adaptive filtering to dynamic weighing of vehicles, Control Engineering Practice 4 (5) (1996) 635–644.
[13] W.-Q. Shu, Dynamic weighing under nonzero initial conditions, IEEE Trans. Instrum. Meas. 42 (4) (1993) 806–811.
[14] R. Kaszyński, J. Piskorowski, Selected structures of filters with time-varying parameters, IEEE Trans. Instrum. Meas. 56 (6) (2007) 2338–2345.
[15] J. Piskorowski, T. Barciński, Dynamic compensation of load cell response: A time-varying approach, Mechanical Systems and Signal Processing 22 (7) (2008) 1694–1704.
[16] P. Pietrzak, Dynamic mass measurement using a discrete time-variant filter, in: Proc. IEEE IEEEI, 2010, pp. 151–155.
[17] J. Nelder, R. Mead, A simplex method for function minimization, The Computer Journal 7 (4) (1965) 308–313.
[18] International recommendation OIML R 76-1, Non-automatic weighing instruments. Part 1: Metrological and technical requirements - Tests (2006).

[19] M. Halimic, W. Balachandran, Y. Enab, Fuzzy logic estimator for dynamic weighing system, in: Proc. IEEE International Conference on Fuzzy Systems, Vol. 3, 1996, pp. 2123–2129.
[20] M. Halimic, A. Halimic, S. Zugail, Z. Huneiti, Intelligent signal processing for electro-mechanical systems, in: Proc. ISMA, 2008, pp. 1–5.
[21] H. Bahar, D. Horrocks, Dynamic weight estimation using an artificial neural network, Artificial Intelligence in Engineering 12 (1-2) (1998) 135–139.
[22] M. Jafaripanah, B. Al-Hashimi, N. White, Application of analog adaptive filters for dynamic sensor compensation, IEEE Trans. Instrum. Meas. 54 (1) (2005) 245–251.
[23] Y. Yamakawa, T. Yamazaki, J. Tamura, O. Tanaka, Dynamic behaviors of a checkweigher with electromagnetic force compensation, in: Proc. XIX IMEKO, 2009, pp. 208–211.